Astronomy Letters, Vol. 28, No. 10, 2002, pp. 701–712. Translated from Pis'ma v Astronomicheskiĭ Zhurnal, Vol. 28, No. 10, 2002, pp. 775–787.

Neutral Hydrogen around the Oxygen-Sequence Wolf–Rayet Star WR 102 and the Nebula G2.4+1.4

I. V. Gosachinskij[1]* and T. A. Lozinskaya[2]

[1]*Special Astrophysical Observatory, St. Petersburg Branch, Russian Academy of Sciences, Pulkovo, St. Petersburg, 196140 Russia*

[2]*Sternberg Astronomical Institute, Universitetskiĭ pr. 13, Moscow, 119992 Russia*

Received May 13, 2002

Abstract—We carried out the first 21-cm line observations of an extended region around the Wolf–Rayet star WR 102 and the associated nebula G2.4+1.4 with the RATAN-600 radio telescope. An irregular H I shell was identified. Its maximum expansion velocity reaches $\sim$50 km s^{-1}, and its outer diameter (at a distance of 3 kpc) is 56 pc. The mechanical luminosity of the stellar wind required to produce the observed shell is estimated to be $\sim 0.8 \times 10^{38}$ erg s^{-1}; the age of the shell is $\sim 3.4 \times 10^5$ yr. We compare the inferred parameters of the H I shell with the structure and kinematics of the ionized nebula and with the dust distribution in the region. © *2002 MAIK "Nauka/Interperiodica"*.

Key words: *interstellar medium, gaseous nebulae; radio sources.*

INTRODUCTION

The effects of strong winds from Wolf–Rayet (WR) stars on the neutral component of the interstellar medium have been studied for several decades. To date, 21-cm H I line observations have been carried out for twenty WR stars and their surrounding nebulae. The first positive result was obtained by Cappa and Niemela (1984), who discovered an H I cavity, 100 pc in diameter, around the star WR 48 (θ Mus). Current observations are performed mostly with the 100-m radio telescope in Bonn (see, e.g., Arnal 1992; Arnal *et al.* 1999) and with the DRAO aperture-synthesis system in Canada (Pineault *et al.* 1996; Arnal 2001). References to the results of other observers who analyzed the H I distribution around WR stars with these instruments can be found in these papers.

H I cavities have been detected more or less reliably around almost all of the WR stars studied. The cavity sizes range from 30 to 100 pc and are oval rather than round in shape. The deficit of gas in cavities compared to the background typically reaches several thousand $M_\odot$. The expansion velocities of the clumpy H I shells around cavities lie within the range 10–15 km s^{-1}, and only for WR 128 did Arnal *et al.* (1999) find the expansion velocity to be 80 ± 22 km s^{-1}.

It should be noted that almost none of the authors detected regular H I shells around cavities with confidence. Virtually all WR stars are greatly displaced from the centers of the associated cavities. When studying the H I region around the star WR 134, Gervais and St Louis (1999) used Hipparcos data to show that the eccentric position of this star in the cavity could be explained by its proper motion.

In several cases, IRAS data also revealed extended dust shells or cavities around WR stars. Extended infrared shells and cavities were found around the nebula NGC 6888 and the star WR 136 (Nichols-Bohlin and Fesen 1993; Marston 1995; Lozinskaya *et al.* 1997), as well as around the stars WR 134 (Pineault *et al.* 1996), WR 125 (Arnal and Mirabel 1991), and WR 140 (Arnal 2001). Goss and Lozinskaya (1995) investigated infrared radiation in the vicinity of two oxygen-sequence WR (WO) stars, including WR 102 discussed here.

The WO stars are of particular interest, because they are rare and possess the strongest winds among the WR stars.

Only six WO stars have been identified among the six hundred WR stars in the Local Group galaxies; three of them, including WR 102, are located in our Galaxy (Van der Hucht *et al.* 1981). According to Barlow and Hummer (1982), the WO stars should be considered as a single sequence that represents the final evolutionary stage of the most massive stars: the final core helium or carbon burning stage.

*E-mail: gos@fsao.spb.su

1063-7737/02/2810-0701$22.00

Since the carbon-burning duration for massive stars is 0.3–1% of the helium-burning duration (Maeder and Meynet 1989), the number of WO stars cannot exceed 1% of the total number of WR stars; i.e., the six known WO stars in the Local Group galaxies form a representative sample. Therefore, studying each of them is of importance in understanding the physics of massive stars and the interaction of stars with the interstellar medium. Moreover, only two of the six known WO stars are associated with bright nebulae; one of these two stars is WR 102 in the nebula G2.4+1.4.

The WO stars are characterized by high-velocity winds, $V \simeq 4500$–7400 km s^{-1} (Barlow and Hummer 1982; Torres *et al.* 1986; Dopita *et al.* 1990; Polcaro *et al.* 1992), and high effective temperatures, 100 000 K (Maeder and Meynet 1989; Dopita *et al.* 1990; Melnick and Heydari-Malayeri 1991).

Optical, infrared, and radio observations of the WR 102 field revealed numerous traces of the action of ionizing radiation and strong stellar wind on the ambient gas.

Images of the nebula G2.4+1.4 in optical lines (Dopita and Lozinskaya 1990; Treffers and Chu 1991) and in radio continuum (Goss and Lozinskaya 1995) clearly reveal a diffuse H II region ionized by the radiation from WR 102 and a thin-filament shell swept up by the wind in this region.

Faint optical filaments were detected far beyond the previously known bright nebula through detailed kinematic studies of the nebula (Dopita and Lozinskaya 1990). The thin-filament shell was shown to be a bubble blown out by the wind at the boundary of a dense cloud. The expansion velocity of the approaching side of the shell is 42 km s^{-1}; no systematic expansion of the far side of the nebula was found. The dense cloud the interaction with which prevents the expansion of the far side of the shell was detected by the radiation of hot dust with a temperature of 30–31 K (Goss and Lozinskaya 1995).

The neutral component of the interstellar medium in the vicinity of WR 102 and the nebula G2.4+1.4 has not yet been studied in 21-cm line emission. Here, we present our 21-cm line observations of an extended region toward WR 102 and G2.4+1.4 in an effort to analyze the H I distribution and kinematics.

INSTRUMENTATION AND TECHNIQUES

To investigate the H I distribution in extended fields around WR 102 and G2.4+1.4, we obtained three drift curves in right ascension at declinations $-26\overset{\circ}{.}8$, $-26\overset{\circ}{.}2$ (the nebula center), and $-25\overset{\circ}{.}6$. The RATAN-600 antenna (Esepkina *et al.* 1979) has an angular resolution of $2.4' \times 50'$ and an effective area of $\sim$900 m^2 at these declinations. An uncooled HEMT amplifier was used at the input (Il'in *et al.* 1997). The system noise temperature was $\sim$70 K, the 39-channel filter spectrum analyzer had a channel bandwidth of 30 kHz (6.3 km s^{-1}), and the separation between channels was 30 kHz (Venger *et al.* 1982). An IBM PC was used for the system control, data acquisition, and preprocessing (Alferova *et al.* 1986).

The drift curve at each declination consisted of two series of three observations (five observations at declination $-26\overset{\circ}{.}2$) each obtained by shifting the receiver tuning frequency by half the channel bandwidth. As a result, each drift curve had 78 spectral channels that followed at 3.15 km s^{-1} intervals in the $\pm$120 km s^{-1} survey band. Independent observations at adjacent radial velocities also allowed the interference to be effectively removed. The antenna-temperature fluctuation rms in spectral channels after averaging the observations over the series was 0.2 K. The antenna and equipment parameters were checked in each series of observations by measuring a set of reference sources (Venger *et al.* 1981).

Subsequently, we subtracted an extended background from the drift curves in each spectral channel by using an upper spatial frequency Fourier filtering code. The Fourier filter passed spatial periods shorter than 192^s ($43'$) virtually without changes and reduced the power of spatial harmonics with periods longer than this boundary by approximately two orders of magnitude. It should be noted that a frequent subtraction of the background component results in underestimation of the brightness and angular size of the remaining small-scale features, because none of the background subtraction methods locates the zero line of the resulting drift curve. In order to take a certain zero line of the drift curves for the subsequent data reduction, we have to rely on a particular model for the cloud structure of the interstellar medium in advance. Since we commonly assume a negative antenna temperature of the line signal (absorption or self-absorption) to be encountered only in a few special cases (see below), it would be reasonable to draw the low-frequency zero line at the lower level of the small-scale antenna-temperature distribution for the H I emission line. The background component of the drift curves subtracted by the above method probably includes the following: (1) large-scale features of the interstellar-gas distribution, such as spiral arms or giant H I complexes; (2) emission from the intercloud medium, if present; (3) small-angular-size features unresolved by the RATAN-600 beam; and (4) a spurious large-scale background produced by far side lobes and the RATAN-600 stray field.

The parameters of H I features were determined in each channel by using a code for Gaussian analysis. In our case, depending on the amplitude threshold

set by the user, this code also separated extended structures into individual Gaussian features. In general, the assumption that the emission from individual clouds is Gaussian in shape appears arbitrary and this should be taken into account when interpreting the results. Next, we established a relationship between H I emission features at adjacent radial velocities and declinations to determine the three-dimensional structure of each H I cloud. Note that a significant subjective factor can also be introduced into this procedure. Therefore, we try to show most of the data in the figures in order that the reliability of identifying particular structures could be estimated.

The measured parameters have the following errors. The radial velocity of an isolated medium-brightness H I feature is measured with an accuracy of at least ± 1 km s^{-1} (in several cases, the accuracy is slightly lower because of the difficulties in separating the object from the background or from neighboring features). The measurement error of the H I line brightness temperature is ± 0.5 K, including the antenna calibration errors. The estimation error of the angular sizes in right ascension is $\pm 0.1^\circ$. In declination, the antenna resolution is much lower and, accordingly, the angular sizes are measured with a lower accuracy.

RESULTS

Continuum and the H I Line

The continuum drift curve of the object is shown in Fig. 1. In contrast to the spectral channels, the Galactic-gas emission background in the 10-MHz-wide continuum channel was drawn by spline interpolation. The following observed parameters of the radio source were obtained:

Right ascension of the brightness peak (1950.0)	$17^h42^m40^s$
Peak antenna temperature	0.23 ± 0.01 K
Half-width of the drift curve	$8'.0 \pm 1.0$
Total flux density at 1.42 GHz	2.65 ± 0.2 Jy

Note that the coordinate and flux density of the source are closely similar to those obtained with the VLA by Goss and Lozinskaya (1995) at a close frequency of 1.49 GHz. The angular size is smaller, because this is the half-width of the brightness distribution integrated over the vertical RATAN-600 beam.

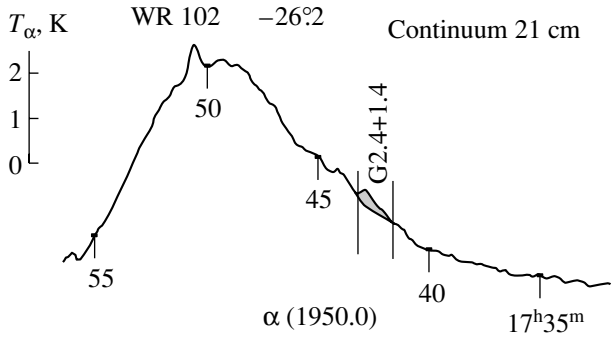

Fig. 1. The continuum drift curve for the G2.4+1.4 region at declination −26°2.

The distribution of H I features after the subtraction of the background radio-line emission is shown in Fig. 2. In this figure, no zero lines of the drift curves are shown (see above for discussion), the radial velocities relative to the local standard of rest are shown on the right, and their range is slightly reduced to save space. The vertical lines in this and succeeding figures drawn at right ascensions 17^h42^m and 17^h43^m correspond to the nebula size at zero radio brightness. The H I features nearest the nebula are hatched.

The Absorption Line and Self-absorption

Before we discuss the possible association of H I clouds with the nebula, we must solve two important problems. First, the object lies near the Galactic center, where the gas column density is high and the differential Galactic rotation is virtually negligible. Second, the well-known self-absorbing H I cloud (see, e.g., Riegel and Crutcher 1972), $30^\circ \times 15^\circ$ in size, is located here at a distance of about 900 pc from the Sun. These factors may lead to features that can be attributed to the absorption line, despite the comparatively low antenna temperature of the source in continuum.

The relative self-absorption is demonstrated by Fig. 3. It shows three H I line profiles that we obtained at the Galactic latitude of the object on three drift curves in right ascension. The interpolated parts of the profiles subjected to self-absorption whose maximum is observed in this region at radial velocities $V(\mathrm{LSR}) = 6-7$ km s^{-1} are hatched. The signal in absorption can be distinguished at the source position in Fig. 4, where the drift curves are shown on a large scale at radial velocities near zero (± 20 km s^{-1}). To reduce noise fluctuations, the drift curves were smoothed over 30^s intervals, which roughly corresponds to the source half-width in continuum. This yielded a fluctuation rms in the spectral channels of 0.1 K (i.e., no more than half the peak antenna temperature of the source in the continuum). In addition,

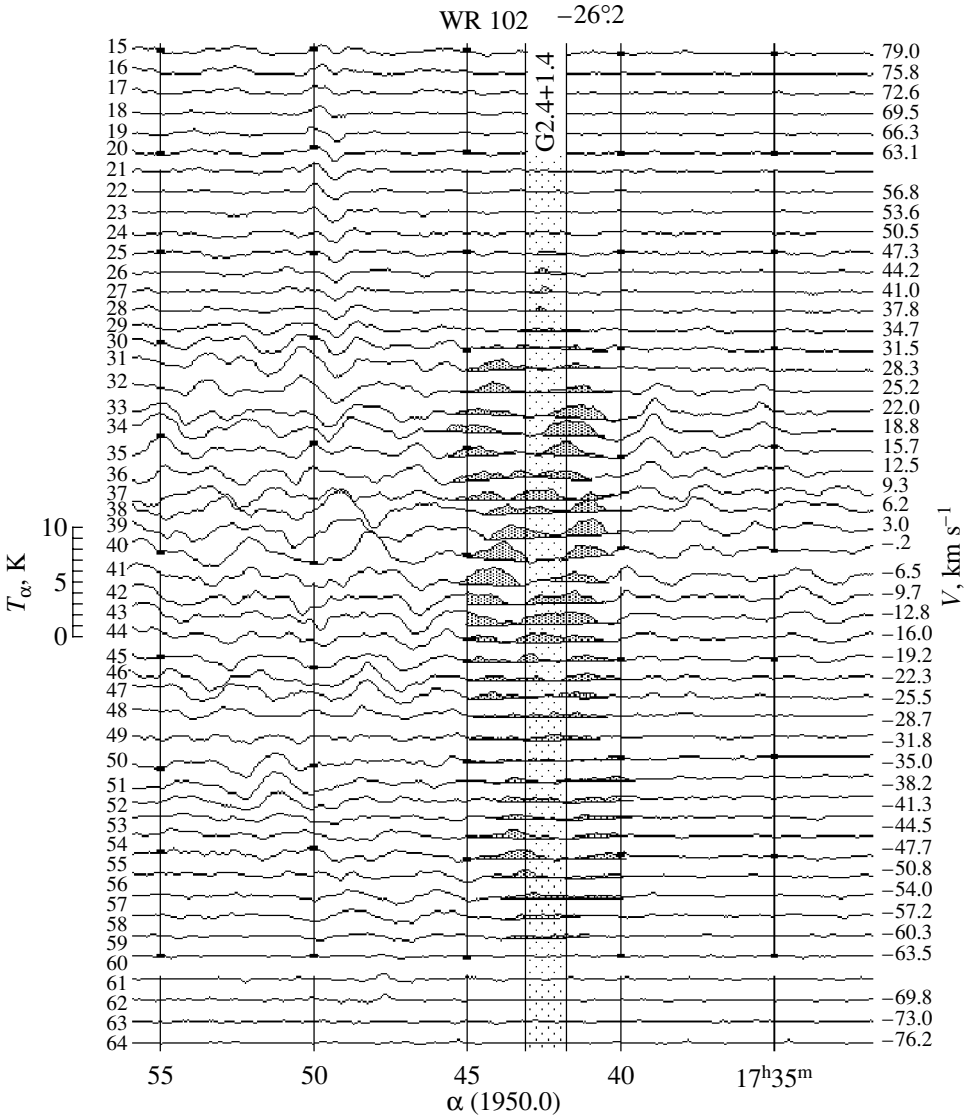

Fig. 2. The drift curves for H I features in the G2.4+1.4 region after the H I background subtraction. No zero lines are shown. Radial velocities relative to the local standard of rest and spectrometer channel numbers are along the right and left vertical axes, respectively. The H I features that may be associated with the observed nebula are hatched.

since one might expect an H I signal of any sign, median zero lines are drawn in the figure. The features with negative antenna temperatures near the source are hatched.

We see from Fig. 4 that there are no signals with negative antenna temperatures at the expected radial velocities at the source position. At the same time, those signals that are marked in the figure cannot correspond to the absorption line, because they do not coincide with the source in coordinates and almost all of them have a depth much larger than its antenna temperature and, in addition, change their positions, depending on radial velocity. Therefore, this kind of structure is attributable not to the absorption line but to an inhomogeneous H I emission background (cloud structure) (accordingly, drawing a median zero line is not appropriate in this case). Background inhomogeneities, which are clearly seen in Fig. 2, "blur" the weaker absorption line from the source. Obviously, it will be impossible to distinguish this line even if the equipment sensitivity is increased significantly.

H I Features Near the Nebula G2.4+1.4

We see from Fig. 2 that the H I clouds immediately adjacent to the nebula G2.4+1.4 are observed over a wide range of radial velocities, from −60 to +50 km s^{-1}. In the range of zero radial velocities (about ±15 km s^{-1}), the large number of background features and their complex shape in the

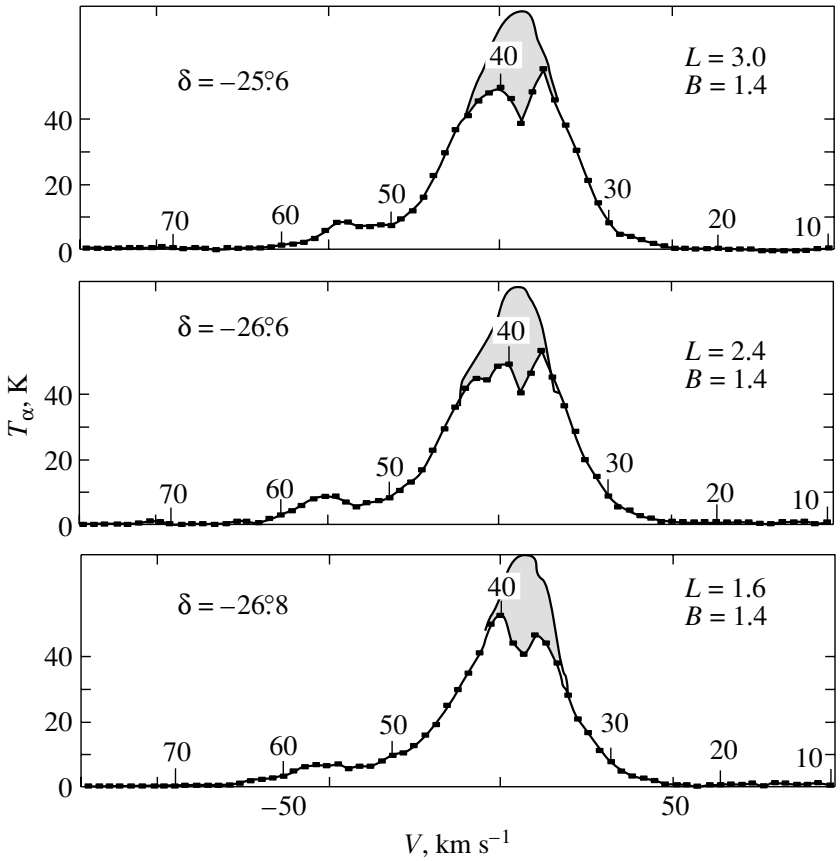

Fig. 3. H I line emission profiles in the G2.4+1.4 region. The parts of the profiles distorted by a self-absorbing H I cloud are hatched.

right ascension–radial velocity plane complicate the identification. To clarify the picture, we performed a Gaussian analysis of the observed drift curves, whose results are shown in Fig. 5. Note that in this procedure, we took a comparatively low threshold for the identification of Gaussian-shaped structures, 0.25 K (i.e., 1σ fluctuations of the spectral drift curves); thus a significant number of noise features are noticeable at high negative and positive radial velocities. Nevertheless, the H I features of significant brightness hatched in the figure reveal a distinct closed structure which may represent an expanding H I shell (provided that it also coincides with the nebula in declination). The latter can be demonstrated in the ranges of radial velocities +15 to +50 km s^{-1} and −15 to −60 km s^{-1}, where there are few background features and the putative shell is identified more clearly.

Figures 6 and 7 show the distribution of H I features in the above ranges of radial velocities on three drift curves in declination. Despite the large vertical RATAN-600 beam, the following conclusions can be drawn from these figures: first, the apparent arc-shaped structures are not displaced in right ascension with changing declination, which would be natural for background Galactic gas structures, and, second, their angular size in right ascension is at a maximum at declination −26.2°, i.e., for the drift curve passing through the center of the optical nebula. Consequently, we may assume with reasonable confidence that the H I ring structure marked in Fig. 5 is actually the expanding shell that immediately surrounds the nebula G2.4+1.4.

It should be emphasized that this assumption undoubtedly requires further confirmation. In particular, high-resolution observations with a circular beam are needed. Indeed, a bright H I feature is observed at the center of our identified shell directly toward the nebula in the velocity range +20 to −13 km s^{-1} (even up to −30 km s^{-1}, but it is fainter here). This is most likely a feature of background gas. However, it may be physically associated with the star WR 102 and the nebula G2.4+1.4 or with an extended arc of dust, because the optical and infrared observations made by Dopita and Lozinskaya (1990) and Goss and Lozinskaya (1995) revealed a rather complex structure and kinematics of the ionized gas and dust near the star (see below). Observations with a circular beam may not give an unequivocal answer either, because we

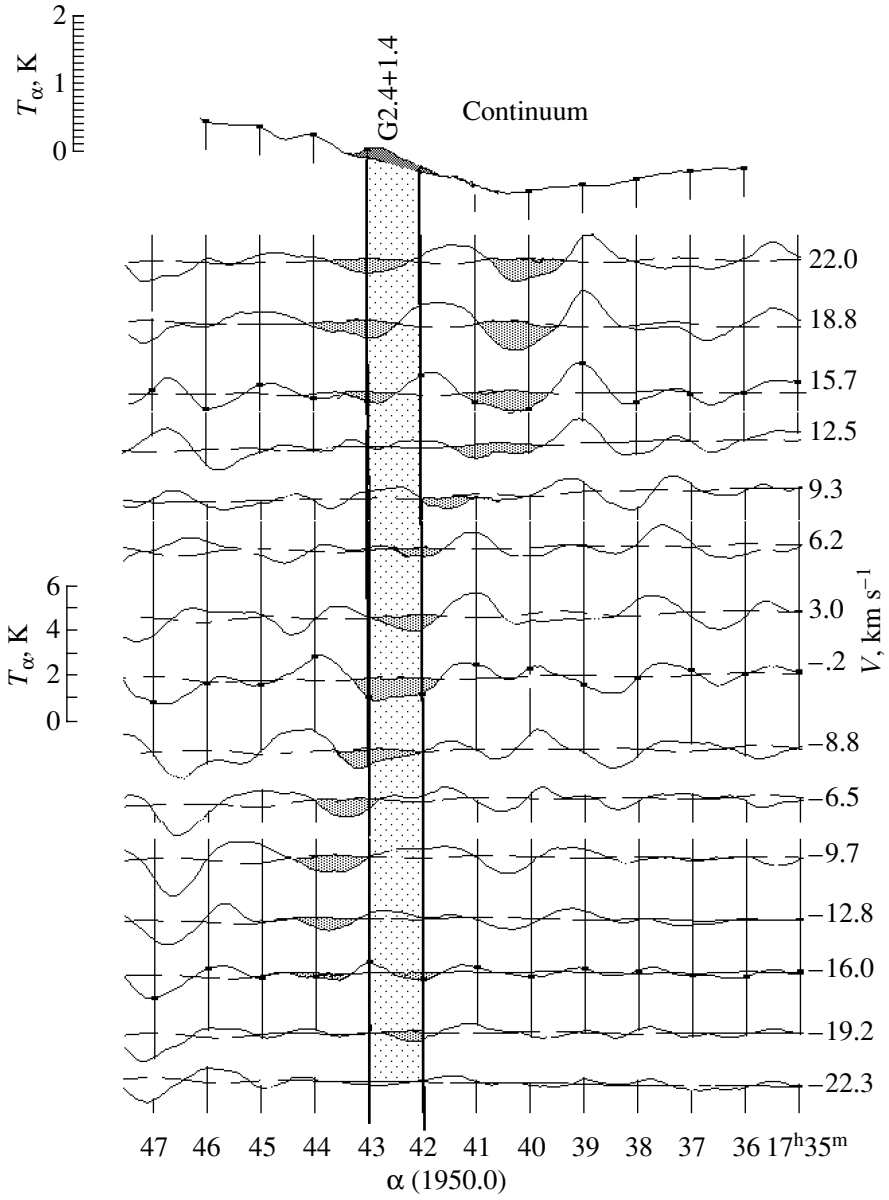

Fig. 4. Parts of the H I drift curves in the G2.4+1.4 region after the H I background subtraction. Zero lines were drawn halfway between the maxima and minima of the features. To reduce noise fluctuations, the curves were smoothed over 30^s intervals in α. The minima that may be associated with H I self-absorption or with the absorption of nebular emission are hatched.

see virtually the entire Galaxy in the 21-cm line at longitude $l = 2.4°$ and the kinematic distances here are uncertain.

Therefore, it should be borne in mind that we determined the parameters of the H I shell given below by assuming that all of the features highlighted in Fig. 5 represent a single expanding shell. In the next section, we also attempt to correlate the observed H I features with the various components of G2.4+1.4 using optical and infrared observations.

Parameters of the H I Shell

Even the mean radial velocity of the shell is difficult to determine. Formally, as the mean value between the most displaced features at positive and negative velocities, it falls within a region of nearly zero values.

Note that Caswell and Haynes (1987) determined the mean radial velocity of the ionized gas, 3 km s^{-1}, and the half-width of internal motions, −53 km s^{-1}, from observations of the H109α and H110α recombination lines in the nebula G2.4+1.4. These data are in good agreement with the observed parameters of the H I shell if it is assumed to immediately surround the nebula.

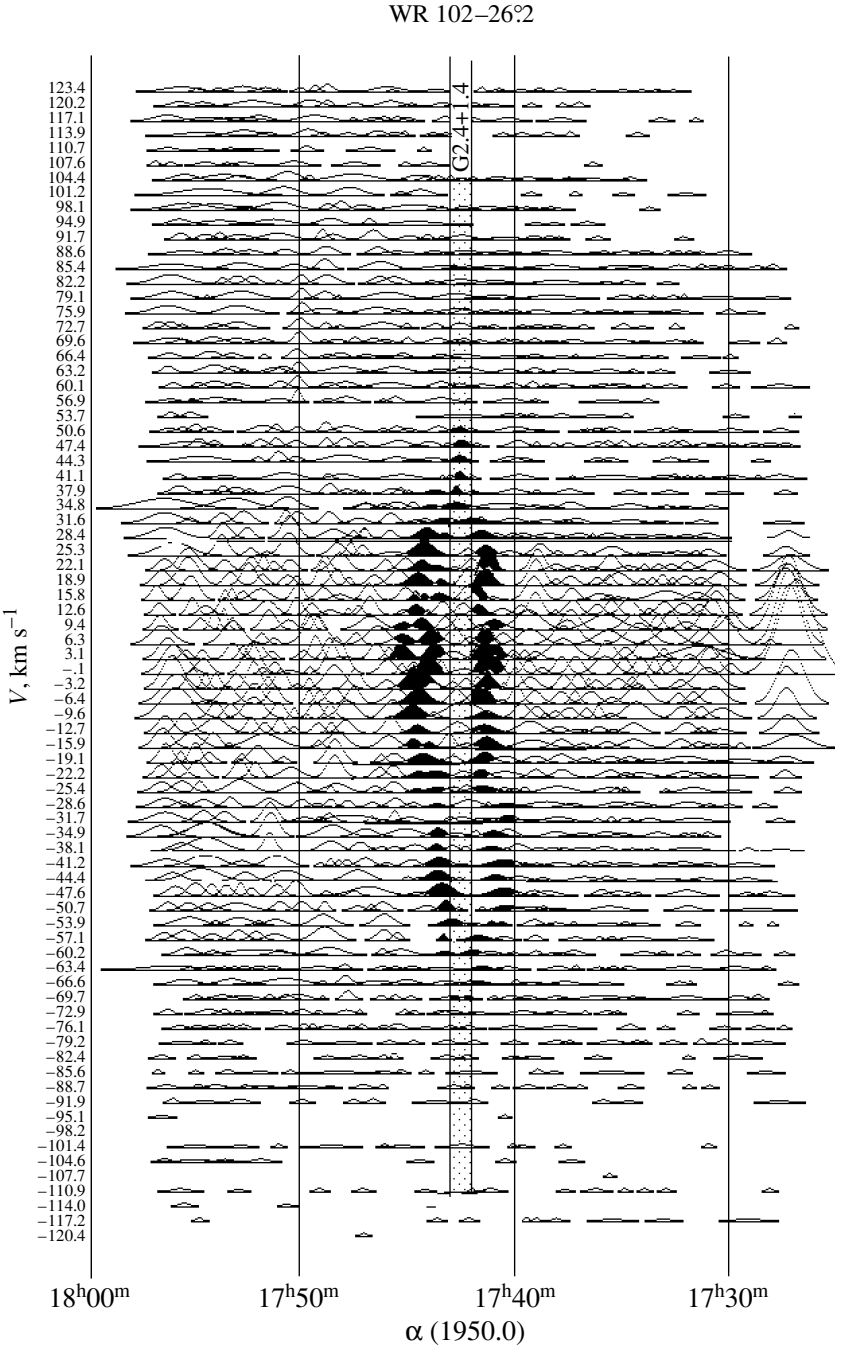

Fig. 5. The drift curves of H I features in the G2.4+1.4 region after a Gaussian analysis of the features whose emission is shown in Fig. 2. The H I features that probably form a single expanding shell around the nebula are hatched.

Optical-line observations revealed bright features in the range of velocities V(LSR) from -20 to $+25$ km s^{-1} (Treffers and Chu 1982; see also references to previous papers therein). Dopita and Lozinskaya (1990) identified the main "nonaccelerated" component of the ionized gas in the nebula at V(LSR) $= +23$ km s^{-1} and the approaching side of the expanding shell whose velocities vary over the range $+15$ to -28 km s^{-1}.

Thus, the velocities of the H I features that we treat here as a manifestation of a single expanding shell around the nebula G2.4+1.4 are generally in agreement with the radio and optical line observations.

We determined the parameters of the H I shell around the H II region G2.4+1.4 after performing a

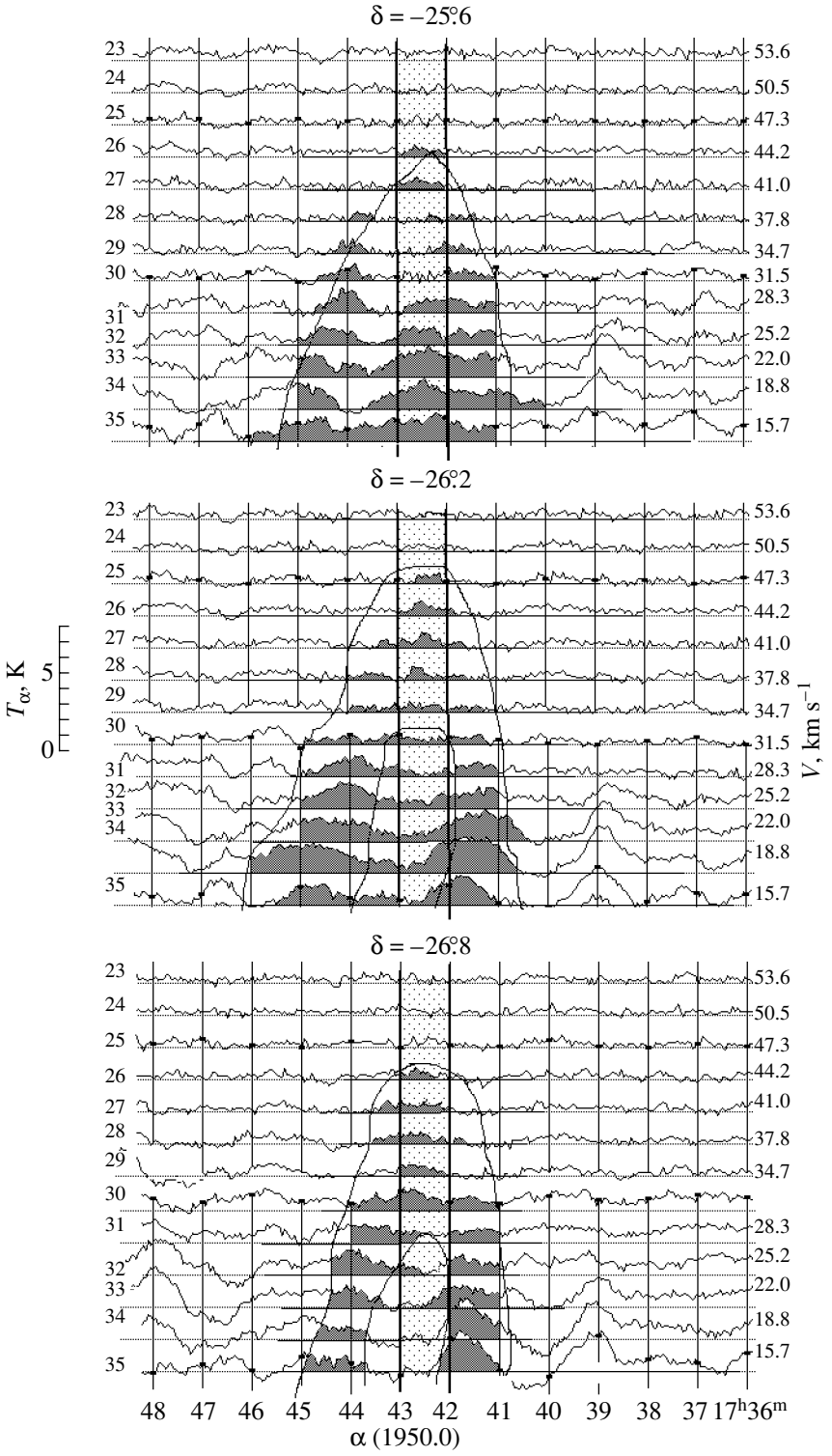

Fig. 6. Part of the putative H I shell at positive radial velocities at three declinations around G2.4+1.4. The positions of the H I features in α at different declinations are not displaced, and the angular size in α is largest at the nebula declination.

Gaussian analysis of the features that were directly obtained from observations. As we mentioned above, our code for Gaussian analysis not only determined the parameters of features but also broke down complex features into individual Gaussians. Some of the data given below differ from their preliminary values calculated from the original observational data

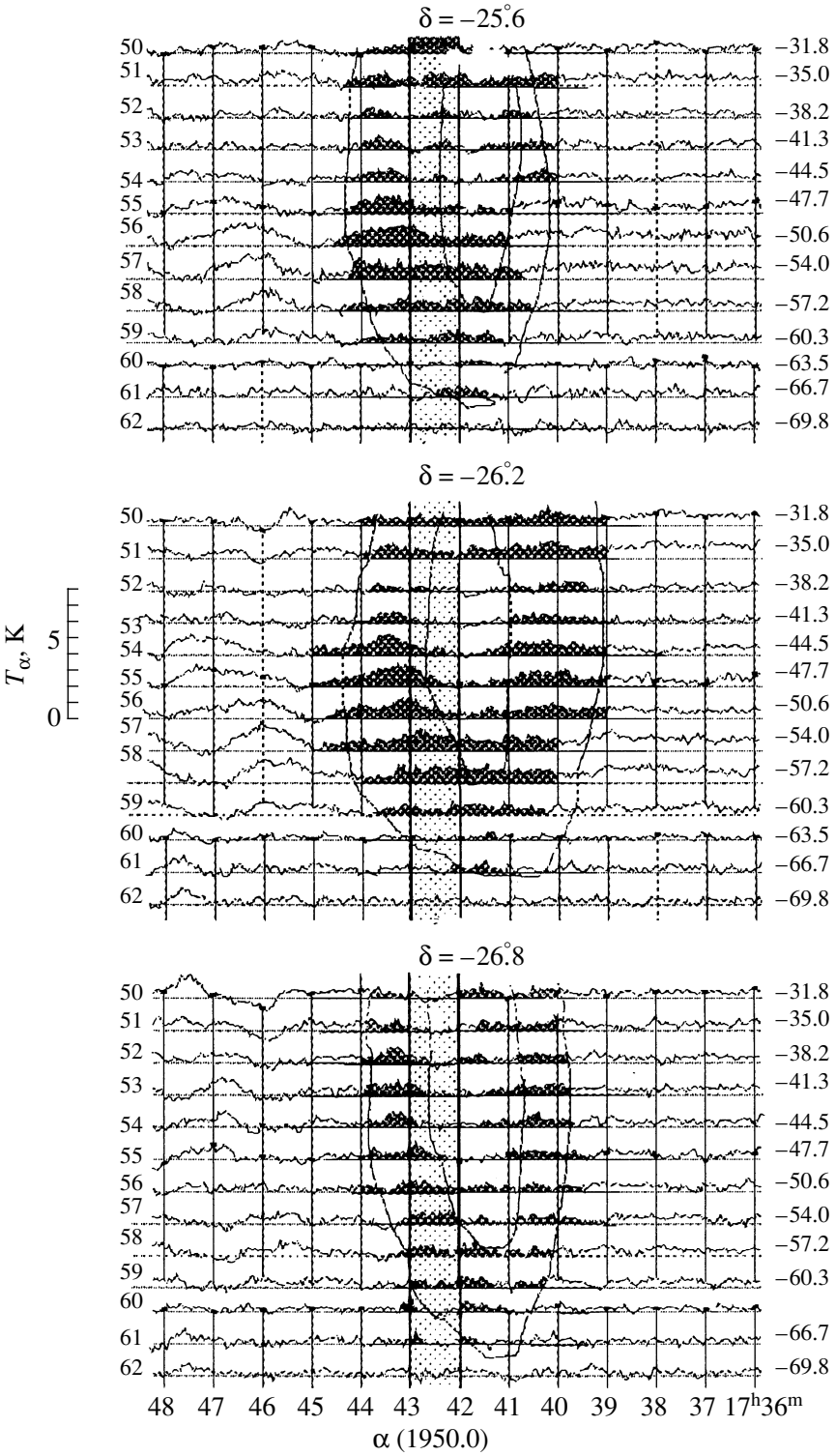

Fig. 7. Same as Fig. 6 for negative radial velocities. The behavior of the features with changing declination is the same as that in Fig. 6.

(Fig. 2) and presented in Gosachinskij and Lozinskaya (2001).

Here, the observed parameters of the H I shell around G2.4+1.4 were determined from the features marked in Fig. 5 by assuming that the shell has a circular symmetry in the plane of the sky.

Coordinates of the center	$\alpha\,(1950) = 17^{\rm h}42^{\rm m}30^{\rm s}$ $\delta\,(1950) = -26\fdg2$
Angular diameter: outer inner	 $1\fdg1$ $0\fdg7$
Mean shell thickness	$\approx 0\fdg2$
Peak line brightness temperature	5.0 ± 0.5 K
Mean Radial velocity	$V(\mathrm{LSR}) = -5 \pm 5$ km s^{-1}
Radial-velocity range	$\Delta V \approx 100$ km s^{-1}

DISCUSSION

The distance to the shell, if it actually surrounds the WO star and the nebula G2.4+1.4, may be taken to be equal to the photometric distance to WR 102 determined by Dopita and Lozinskaya (1990): $d = 3 \pm 1$ kpc.

Assuming a uniform gas density distribution within the shell, we obtain the following parameters of the H I shell at a distance of 3 kpc

Maximum expansion velocity	≈ 50 km s^{-1}
Outer diameter	56 pc
Inner diameter	37 pc
H I density	≈ 2.7 cm^{-3}
H I shell mass	$4.2 \times 10^3\ M_\odot$

We find the ambient gas density in the region under the common assumption that the entire gas of the shell was initially uniformly distributed over its observed volume: $n_0 = 1.85$ cm^{-3}.

According to the optical studies by Dopita and Lozinskaya (1990), the swept-up shell is a bubble blown out by the wind from the star located at the boundary of a dense cloud facing the observer: the density inside and outside the cloud is $n_0 \simeq 60$ cm^{-3} and $n_0 \simeq 3$–4 cm^{-3}, respectively. As we see, the H I density is close to the gas density outside the cloud inferred from optical observations. This is quite natural if the dense cloud is comparable in size to the nebula, because our derived H I density was averaged over the large (in height) RATAN-600 beam.

The H I structure marked in Fig. 5 is not a perfect ring. We can interpret the H I structures observed in the coordinate–velocity plane in more detail and can attempt to compare them with the results of optical and infrared studies.

Three barrel-shaped groups of bright H I features, each showing evidence of an expanding shell structure, can be distinguished at declination $-26\fdg2$:

I—the central velocity $V(\mathrm{LSR}) = 15.2$–18 km s^{-1}; the velocity range is $V(\mathrm{LSR}) = 6.3$–9.4 km s^{-1} to $V(\mathrm{LSR}) = 35$–44 km s^{-1};

II—the central velocity $V(\mathrm{LSR}) = -3 \ldots -9$ km s^{-1}; the velocity range is $V(\mathrm{LSR}) = 6.3$–9.4 km s^{-1} to $V(\mathrm{LSR}) = -20 \ldots -28$ km s^{-1};

III—the central velocity $V(\mathrm{LSR}) = -45 \ldots -47$ km s^{-1}; the velocity range is -28 to -57 km s^{-1}.

Most of the features distinguished on the drift curves in the coordinate–velocity plane may be assumed (with all of the above reservations) to be associated with G2.4+1.4 and WR 102. Indeed, previous 21-cm line observations for a large number of WR stars (see Introduction) showed that most WR stars are associated with cavities or shells of neutral gas revealing complex (clumpy) structures and kinematics.

As for the object under study, optical, radio, and infrared observations suggest a nonuniform distribution of ionized gas and dust in extended regions around the star WR 102. Detailed optical (Dopita and Lozinskaya 1990; Treffers and Chu 1991) and radio (Goss and Lozinskaya 1995) studies of the structure and kinematics of G2.4+1.4 clearly reveal a diffuse H II region ionized by the star WR 102 and a thin-filament shell in this region swept up by the wind. The size of the H II region at the $ME = 300$ level is $16'$ (14 pc); the shell size is $10'$ (10 pc). The expansion velocity of the approaching side of the shell is 42 km s^{-1}, with the far side showing no systematic expansion.

Such kinematics of the optical nebula suggests that there must be a dense cloud collision with which slowed down the expansion of the receding side of the shell. This cloud of hot dust was detected by Goss and Lozinskaya (1995) through the reduction of archival IRAS data. The morphology of the bright infrared source follows the shape of the thermal radio source and the bright part of the nebula. A map of the distribution of the dust temperature determined from the IRAS (60)/(100) flux ratio indicates that the highest dust temperature in the large region is observed in this bright source, suggesting that the star WR 102 is physically associated with the dense cloud. A large-scale map of the infrared brightness distribution also reveals an extended lagoon surrounded by a weak shell structure in the west [see Fig. 6 from Goss and Lozinskaya (1995)]. The lagoon size is about $30'$; WR 102 and its optical/radio/infrared nebula are located at the northwestern boundary of the lagoon, on the spur bounding it.

Given the above optical and infrared observations, the identified structures in the H I distribution can be interpreted as follows.

Group I of H I features at $V(\mathrm{LSR}) = 15.2$–18 km s^{-1} may represent mainly the nonaccelerated neutral gas in the region. Since the star lies at the forefront of the dense cloud, the difference from the velocity of the wind-nonaccelerated ionized gas in

G2.4+1.4 [$V(\mathrm{LSR}) = 23 \pm 5$ km s^{-1}]), as inferred by Dopita and Lozinskaya (1990), can be explained by expansion of the H II region into the cloud at the speed of sound.

Group II of H I features at $V(\mathrm{LSR}) = -3 \ldots -9$ km s^{-1} may be correlated with bright filaments of the swept-up ionized shell [according to Dopita and Lozinskaya (1990), the mean velocity of the brightest optical filaments on the approaching side of the shell is -5 km s^{-1}]. If we make the common assumption that the ambient gas has a two-component structure (dense cores in a less dense diffuse medium), then we can naturally explain the presence of bright, weakly accelerated ionized filaments and dense H I cloudlets at similar velocities that we combined into structure II and those features that are observed as separate clouds in projection onto G2.4+1.4 at velocities from +25 to -30 km s^{-1} (see Fig. 5). The latter can also be associated with the neutral gas in the dust arc mentioned above, which is projected onto the nebula in the coordinate–velocity plane when observed with a knife-edge beam.

The velocities of our identified H I structure III (the central velocity is $V(\mathrm{LSR}) = -45 \ldots -47$ km s^{-1}) closely match the highest negative velocities of faint optical filaments on the approaching side of the shell swept up by the wind.

Of course, a detailed comparison of this kind requires 21-cm line observations with a circular diagram. For now, we can only conclude that the observed H I features at all of the mentioned velocities can be naturally explained in terms of the model of a bubble at the boundary of a dense cloud (Dopita and Lozinskaya 1990) and, accordingly, can be combined into a single H I shell surrounding the WO star and G2.4+1.4.

Using the standard relations for a cavity swept up by stellar wind that follow from the classical theory by Weaver *et al.* (1977),

$$R(t) = 66 n_0^{-1/5} L_{38}^{1/5} t_6^{3/5} \text{ pc},$$

$$v(t) = 39 n_0^{-1/5} L_{38}^{1/5} t_6^{-2/5} \text{ km s}^{-1}$$

(here, R is the radius of the shell, v is its expansion velocity, t_6 is its age in Myr, and L_{38} is the stellar-wind mechanical luminosity in units of 10^{38} erg s^{-1}), we find the required stellar-wind mechanical luminosity and the shell age:

$$L_w = 0.8 \times 10^{38} \text{ erg s}^{-1}, \quad t = 3.4 \times 10^5 \text{ yr}.$$

The required stellar-wind mechanical luminosity derived from the parameters of the H I shell is lower than the WO wind mechanical luminosity inferred by Dopita *et al.* (1990) and Dopita and Lozinskaya (1990) from the observations of WR 102: $L_w = 2 \times 10^{38}$ erg s^{-1} at the wind velocity $V_w = 5500$ km s^{-1}.

At the same time, our derived kinematic age of the H I shell, $t = 3.4 \times 10^5$ yr, is an order of magnitude longer than the duration of the WO stage (the spectrum of WR 102 and its position in the Hertzsprung–Russell diagram suggest a stage close to the bare CO core of a high-mass main-sequence star: $M_{\mathrm{init}} = 40$–$60 M_\odot$ (Dopita *et al.* 1990). This indicates that the wind from the star at the preceding WN and WC stages also determines the structure of the surrounding H I shell.

According to our data, the total kinetic energy of the H I shell determined by its mass and velocity is $E_{\mathrm{kin}} \simeq 1.3 \times 10^{50}$ erg. This value is much lower than the total mechanical energy supplied by the wind from the central star over the shell lifetime even if it is considered that the mechanical luminosity of the wind from the WR star at the WN and WC stages can be a factor of 4 or 5 lower than that at the final WO stage.

Note also that there is every reason to expect that the structure and kinematics of the ambient neutral gas are determined by the action of the WO star and its progenitor at all stages, including the main-sequence stage.

CONCLUSIONS

We have presented the RATAN-600 21-cm line observations of the fields around the star WR 102 and the associated nebula G2.4+1.4. The neutral component of the interstellar medium near WR 102 has not been studied previously in 21-cm line emission.

We identified H I features in the right ascension–radial velocity plane which form a ring structure of neutral hydrogen immediately surrounding the nebula G2.4+1.4. We argue that this structure can represent an extended expanding shell of neutral gas around the WO star.

The identified H I shell has an irregular structure. Its outer and inner diameters are 1°.1 or 56 pc and 0°.7 or 37 pc, respectively, for the assumed photometric distance to the star of 3 kpc.

Based on the idealized model of a spherically symmetric shell of uniform density, we determined the mean H I density in the shell, ≈ 2.7 cm^{-3}, and the total H I mass, $4.2 \times 10^3\ M_\odot$. If the entire gas of the shell is initially uniformly distributed over its observed volume, then the mean ambient gas density in the region is $n_0 = 1.85$ cm^{-3}.

The H I features that we treat as a single shell structure are observed over a wide range of radial velocities: $\Delta V \approx 100$ km s^{-1}; the mean radial velocity

is $V(\mathrm{LSR}) = -5 \pm 5$ km s^{-1}; the maximum shell expansion velocity reaches $\approx$50 km s^{-1}.

It should be emphasized that the assumption that the H I features form a single structure representing an expanding shell undoubtedly requires further confirmation. High-resolution observations with a circular beam are primarily needed. Nevertheless, comparison of the results of our 21-cm line observations with the structure and kinematics of the ionized nebula G2.4+1.4 inferred from the optical observations of Dopita and Lozinskaya (1990) and with the dust distribution in the region inferred from the data of Goss and Lozinskaya (1995) suggests that the derived parameters of the H I shell are consistent with the model of a bubble blown out by the wind from a WO star at the boundary of a dense cloud adopted in these studies.

Based on the standard theory for the interaction of a strong stellar wind with the interstellar medium, we estimated the mechanical luminosity of the stellar wind required for the observed H I shell to be formed, $L_w \sim 0.8 \times 10^{38}$ erg s^{-1}, and the shell age, $t = 3.4 \times 10^5$ yr. Similar mechanical luminosity and duration of the stellar wind were obtained by Dopita and Lozinskaya (1990) through a detailed analysis of the structure and kinematics of the thin-filament optical nebula G2.4+1.4. Spectroscopic observations of the central star (Dopita *et al.* 1990) suggest that mass loss at the WR and WO stages provides such a wind mechanical luminosity. Thus, comprehensive optical, infrared, radio-continuum, and 21-cm line observations of the WR 102 field revealed numerous traces of the action of ionizing radiation and strong WO stellar wind on the ambient gas.

ACKNOWLEDGMENTS

We wish to thank G.N. Il'in, Z.A. Alferova, and T.V. Monastyreva from the Special Astrophysical Observatory for maintaining the equipment in an operational state and for help in the observations. This work was supported by the Russian Foundation for Basic Research (project nos. 01-02-17154 and 01-02-16118).

REFERENCES

1. Z. A. Alferova, I. V. Gosachinskij, S. R. Zhelenkov, and A. S. Morozov, Izv. SAO **23**, 89 (1986).
2. E. M. Arnal, Astron. Astrophys. **254**, 305 (1992).
3. E. M. Arnal, Astron. J. **121**, 413 (2001).
4. E. M. Arnal and I. F. Mirabel, Astron. Astrophys. **250**, 171 (1991).
5. E. M. Arnal, C. E. Cappa, J. R. Rizzo, and S. Cichowolski, Astron. J. **118**, 1798 (1999).
6. M. J. Barlow and D. C. Hummer, in *Proceedings of the IAU Symposium No. 99 "Wolf-Rayet Stars: Observations, Physics, Evolution," Cozumel, Mexico, 1981,* Ed. by C. W. H. de Loore and A. J. Willis (D. Reidel, Dordrecht, 1982), p. 387.
7. C. Cappa de Nicolau and V. S. Niemela, Astron. J. **89**, 1398 (1984).
8. J. L. Caswell and R. F. Haynes, Astron. Astrophys. **171**, 261 (1987).
9. M. Dopita and T. A. Lozinskaya, Astrophys. J. **359**, 419 (1990).
10. M. A. Dopita, T. A. Lozinskaya, P. J. McGregor, and S. J. Rawlings, Astrophys. J. **351**, 563 (1990).
11. N. A. Esepkina, N. S. Bakhvalov, B. A. Vasil'ev, *et al.*, Izv. SAO **11**, 182 (1979).
12. S. Gervais and N. St-Louis, Astron. J. **118**, 2394 (1999).
13. I. V. Gosachinskij and T. A. Lozinskaya, in *Proceedings of the All-Russia Astronomical Conference* (Sankt-Peterb. Gos. Univ., St. Petersburg, 2001), p. 51.
14. W. M. Goss and T. A. Lozinskaya, Astrophys. J. **439**, 637 (1995).
15. K. A. van der Hucht, P. S. Conti, I. Lundstrom, and B. Stenholm, Space Sci. Rev **28**, 227 (1981).
16. G. N. Il'in, A. M. Pilipenko, and V. A. Prozorov, in *Proceedings of the XXVII Radio-astronomical Conference* (IPA RAN, St. Petersburg, 1997), p. 128.
17. T. A. Lozinskaya, V. V. Pravdikova, I. V. Gosachinskij, and S. A. Trushkin, Astron. Zh. **74**, 376 (1997) [Astron. Rep. **41**, 327 (1997)].
18. A. Maeder and G. Meynet, Astron. Astrophys. **210**, 155 (1989).
19. A. P. Marston, Astron. J. **109**, 2257 (1995).
20. J. Melnick and M. Heydari-Malayeri, in *Proceedings of the IAU Symposium No. 143 "Wolf-Rayet Statrs and Inerrelations with Other Massive Stars in Galaxies,* Ed. by K. A. van der Hucht and B. Hidayat (Kluwer, Dordrecht, 1991), p. 409.
21. J. Nichols-Bohlin and R. A. Fesen, Astron. J. **105**, 672 (1993).
22. S. Pineault, S. Gaumont-Guay, and B. Madore, Astron. J. **112**, 201 (1996).
23. V. F. Polcaro, R. Viotti, C. Rossi, and L. Norci, Astron. Astrophys. **265**, 563 (1992).
24. K. W. Riegel and R. M. Crutcher, Astron. Astrophys. **18**, 55 (1972).
25. A. V. Torres, P. S. Conti, and P. Massey, Astrophys. J. **300**, 379 (1986).
26. R. R. Treffers and Y.-H. Chu, Astrophys. J. **254**, 132 (1982).
27. R. R. Treffers and Y.-H. Chu, Astrophys. J. **366**, 181 (1991).
28. A. P. Venger, I. V. Gosachinskij, V. G. Grachev, and N. F. Ryzhkov, Izv. SAO **14**, 118 (1981).
29. A. P. Venger, V. G. Grachev, T. M. Egorova, *et al.*, Soobshch. SAO, No. 35, 5 (1982).
30. R. Weaver, R. McCray, J. Castor, P. Shapiro, and R. Moore, Astrophys. J. **218**, 377 (1977).

Translated by V. Astakhov